ISBN: 978-3-95450-214-1 ISSN: 2673-5490 doi:10.18429/JACoW-IPAC2021-WEPAB189

EIC HADRON BEAMLINE VACUUM STUDIES*

D. Weiss†, S. Verdú-Andrés‡, M. Mapes, J. Tuozzolo
Brookhaven National Laboratory, Upton, NY, USA

Abstract

Ninety percent of the EIC hadron ring vacuum chamber consists of cold-bore sections running through and interconnecting 4.55 K RHIC superconducting (SC) magnets. The EIC operating specification requires shorter bunches and 3x higher intensity beams which are not appropriate for the present RHIC stainless steel cold-bore beam tube. The intensity and emittance of the hadron beams will degrade due to interactions with residual gas or vacuum instabilities arising from the expected resistive-wall (RW) heating, electron clouds, and beam-induced desorption mechanisms. Without strategies to limit RW heating, major cryogenic system modifications are needed to prevent SC magnet quenches. The SC magnet cold-bore beam tubes will be equipped with a high RRR copper-clad stainless steel screen to significantly reduce RW heating and so the effect on the SC magnet cryogenic heat load and temperature. A thin amorphous carbon film applied to the beam-facing copper surface will suppress electron cloud formation. This paper discusses the vacuum requirements imposed by the EIC hadron beams and the plans to achieve the necessary vacuum and thermal stability that ensure acceptable beam quality and lifetime.

INTRODUCTION

The hadron storage ring (HSR) of the BNL's Electron-Ion Collider (EIC) will use part of the two hadron storage rings of the Relativistic Heavy Ion Collider (RHIC) [1]. The EIC hadron beamlines will host bunched beams of protons, light and heavy ions up to uranium at energies varying from 25 to 275 GeV/nucleon. The intensity and emittance of the hadron beams can degrade over time due to beam interactions with residual gas in the vacuum chambers and from instabilities arising from resistive-wall heating, beam-induced desorption mechanisms and electron cloud. Ensuring a low operating pressure and stable beam vacuum wall surfaces in the EIC hadron beamlines are thus important to maximize the useful beam lifetime.

About 90% of the hadron beamline runs through sections of interconnected superconducting magnets operating at 4.55 K (i.e., the cold bore), with the remaining being ambient temperature sections. A sketch of the EIC hadron beamline vacuum system is shown in Fig. 1. The shorter, higher intensity bunches of the EIC impose cold bore beamline modifications in order to guarantee adequate cold bore vacuum conditions. The planned modifications consist of beam screens for the beam pipe of each superconducting magnet, the striplines located in the magnet interconnects and RF-shielded bellows, as well as new beam position monitors [2]. Beam screens will be constructed from high RRR copper clad stainless steel sheet material formed to provide sufficient beam aperture and thermal contact with the magnet cold bore. Additionally, the beam facing screen surface will be sputter coated with amorphous carbon (a-C). Compared to the bare stainless steel superconducting magnet beam tube, the RRR copper significantly reduces the resistive-wall heating, hence the dynamic heat load to the 4.55 K magnets. The a-C coating is intended to suppress electron cloud buildup thanks to its low secondary electron yield and with its high adsorption capacity may improve cryogenic vacuum performance dependent on the screen temperature.

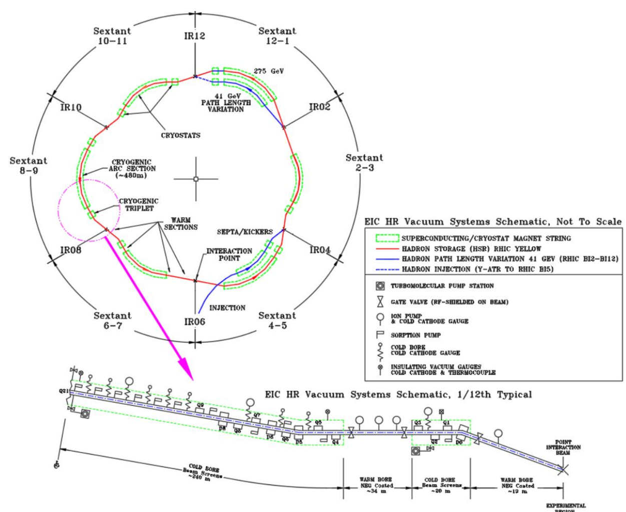

Figure 1: Sketch of the EIC hadron beamline system.

VACUUM LEVEL REQUIRED TO LIMIT BEAM-GAS INTERACTION

Reference [3] discussed the vacuum level required in the warm and cold sections of RHIC to limit the beam lifetime and emittance growth of the 110 GeV $^{197}Au^{79+}$ beam. Heavy ion beams will show larger beam loss rates given the larger cross section of the heavy ion nuclei. The study assumed a pressure of 5×10^{-10} Torr in the warm section (300 K), with a gas composition of 90% H_2, 5% CH_4 and 5% CO and a pressure of 1×10^{-11} Torr in the cold section (5 K) with 100 % He. Keeping the pressure below those values would guarantee about 600 h of beam lifetime in the warm section and 240 h in the cold section. While the EIC HSR will have a longer cold section than the 80% used for the RHIC estimate, the pressure level stipulated for RHIC still provides 214 h lifetime in the cold section of the EIC and, as the warm section is reduced, 1200 h in the warm section.

* Work supported by Brookhaven Science Associates, LLC under Contract No. DE-SC0012704 with the U.S. Department of Energy.
† weiss@bnl.gov
‡ sverdu@bnl.gov

ISBN: 978-3-95450-214-1 ISSN: 2673-5490 doi:10.18429/JACoW-IPAC2021-WEPAB189

Since 2012 RHIC has 3D operational stochastic cooling for ion beams [4], which is also in the EIC HSR baseline. As lower energy beams suffer faster emittance growth, the focus now is placed on the 41 GeV proton beam of the EIC. With a normalized vertical emittance of 0.45 mm mrad, the emittance growth lifetime can be more than 200 h if the pressure in the cold sections is kept under the threshold already defined for the cold sections of RHIC (Fig. 2).

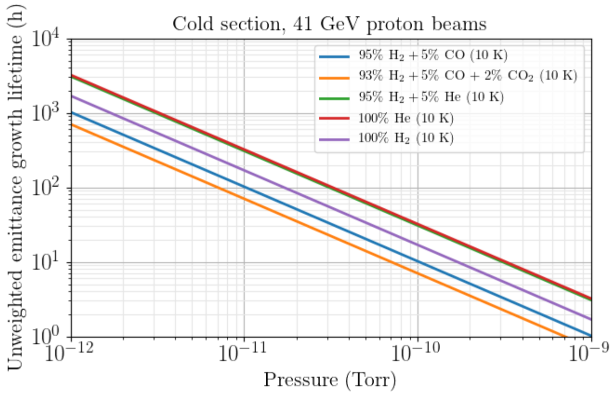

Figure 2: Unweighted emittance growth lifetime for the 41 GeV proton beam in the cold section of RHIC versus pressure.

VACUUM STUDIES

A first study estimates the expected pressure of the beamline at cold based on the average pressure routinely achieved in the RHIC superconducting arcs with the existing ion pumps and assuming a certain adsorption coverage subsequent to cooldown. Subsequent analysis evaluates the impact of increasing gas density originated at warm-to-cold transitions and magnet interconnects, under the assumption that the a-C film successfully suppresses e-cloud.

Initial Conditions

Early in the RHIC program the cold bore was roughed down with sorption and turbo pumps to $\leq 10^{-3}$ Torr prior to cooldown. Operation with higher intensity beams encountered e-cloud and pressure instabilities. Different mitigation countermeasures were implemented, like adding ion pumps to reduce the beamline vacuum level prior to cool down [5]. Figure 3 shows an average pressure prior to cooldown of about 1×10^{-6} Torr achieved with assistance from the ion pumps. Assuming cooldown to 4 K and all gas adsorbed, this pressure level is low enough to result in less than a monolayer of H_2 on the RHIC stainless steel beam tube surface, thus reducing e- cloud susceptibility. The pressure post cooldown is in the 10^{-10} Torr range as measured by a gauge located after a long conduit at ambient temperature, so the actual beamline pressure is lower.

Taking now the adsorption capacity of 2×10^{17} H_2/cm^2 measured for amorphous carbon at COLDEX [6], the initial coverages in the 69 mm-diameter stainless-steel beam tubes of the RHIC superconducting arcs (assumed to be at 4 K)

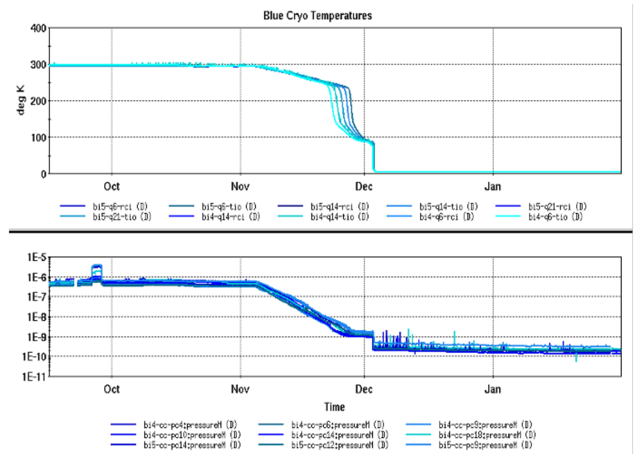

Figure 3: Vacuum as a function of the magnet temperature during cooldown prior to a recent RHIC run.

is expected to be an even smaller fraction of a monolayer. For the case of a beam screen coated with a thin a-C film and kept at a temperature not higher than 10 K, the resulting monolayer coverage is about 100x lower than RHIC. Using the measured adsorption isotherm of a-C at 10 K, the saturation vapor pressure at such low monolayer coverage is less than 1×10^{-11} Torr, or 2×10^{6} H_2/cm^3, a full order of magnitude lower than current RHIC conditions and definitely low enough to satisfy the beam lifetime goal.

Time Dependent 1-D Vacuum Study

Following cooldown, gas sourced from the warm-to-cold transitions at the ends of the arcs, magnet interconnects and leaks can increase the gas density. These conditions are evaluated as a propagating wave dependent on the a-C film adsorption isotherm and beamline conductance. The a-C adsorption isotherm is considered a function of the beam screen temperature (static and operating). The COLDEX experiment finds that physical adsorption by the a-C film starts below 35 K for H_2 and 80 K for CO. The cryosorption capacity for H_2 is 1×10^{15} H_2/cm^2 at 35 K and 2×10^{17} H_2/cm^2 for temperatures below 10 K [6]. This suggests about 100x adsorption capacity for H_2 compared to typical UHV prepared metallic surfaces, which is assumed in the initial study presented herein.

Figure 4 depicts an EIC arc magnet section with interconnected dipole and CQS magnets. Along the beamline, at each interconnect, there are RF-shielded bellows and either a sorption pump loaded with 300 grams of activated charcoal or a gauge conduit. The worst case scenario presented excludes the sorption pumps from the analysis.

The 1-D wave propagation analysis models the gas source at one interconnect and, considering a symmetric system, calculates the time for the wave to reach the midpoint of the magnet. The 1-D wave model [7] assumes that H_2 gas ($2Q$) has the same probability of moving in either direction away from the source location, $x_0 = 0$. Initially hydrogen is strongly adsorbed by a narrow band dx of the cold bore wall

ISBN: 978-3-95450-214-1 ISSN: 2673-5490 doi:10.18429/JACoW-IPAC2021-WEPAB189

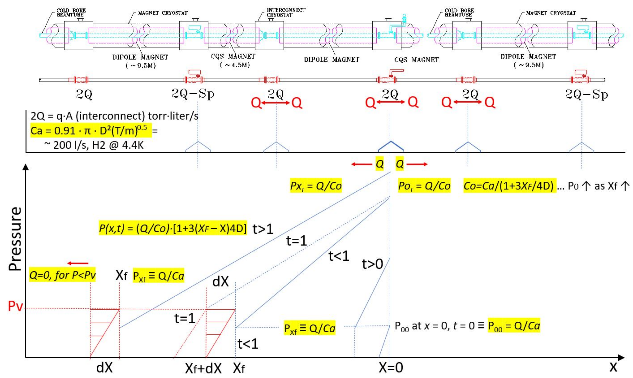

Figure 4: Sketch of the 1-D wave propagation model for one section of a EIC superconducting arc.

at the source. With the buildup of hydrogen on the surface, the adsorption-desorption process will reach an equilibrium and becomes that of the adsorption isotherm. Only then will the leading edge of the pressure zone progress down the beamline to be adsorbed by the 'fresh' band of the a-C screen at the leading edge of the wave front. This process is shown in Fig. 4. The total gas pumped by the magnet cold bore from the source, $x_0 = 0$, to the gas wave front x_f is obtained via integration of the adsorption isotherm relation $\theta(x)$ as follows:

$$Q_t = k_2 \int_0^{x_f} \theta(x)\, dx, \tag{1}$$

where $k_2 = \pi \sigma_m r D T / N_0$ and σ_m is the monolayer coverage at temperature T, r is the surface roughness factor, D is the beam tube diameter and N_0 is Avogadro's number. For integration purposes, the power law approximation of the adsorption isotherm relation is used here, with the surface coverage defined as $\Theta = k_1 P^m$. We get:

$$Q_t = k_1 k_2 \int_0^{x_f} [P(x)]^m\, dx, \tag{2}$$

where the pressure variation along x, assumed linear due to constant outgassing rate Q and aperture C_a, is written as:

$$P(x) = \frac{Q}{C_a}\left[1 + 0.75\frac{(x_f - x)}{D}\right]. \tag{3}$$

Combining Eqs. (2) and (3) and solving the integral finds:

$$Q_t = -k_1 k_2 \left(\frac{Q}{C_a}\right)^m \frac{D}{0.75\,(m+1)}\left[1 - \left(1 + 0.75\frac{x_f}{D}\right)^{m+1}\right]. \tag{4}$$

The time for the wave to propagate a distance x_f is $t_f = Q_t/Q$. Table 1 presents the time t_f it takes for the H_2 gas wave to reach the middle of the RHIC arc dipole, $x_f = 5$ m, for various interconnect and cold bore conditions, estimated using the 1-D wave model. Case I is the current RHIC chamber, using adsorption isotherms from [7]. Cases II and III assume that the chamber is covered with a-C film at 11 K and 6.5 K, respectively, using data from [6]. All cases use r = 1. The average gas density at t_f is given by ρ_{avg}. Assuming no leaks, the time for the average gas to reach the threshold limiting beam lifetime exceeds, in many cases, several years. Machine warm-ups, when adsorbed gas accumulated during machine operation will desorb and be removed by the ion pumps, are expected on a yearly basis.

Table 1: Time for the H_2 Gas Wave To Reach the Middle of the Rhic Arc Dipole in Function of Interconnect and Cold Bore Characteristics

Interconnect Thermal			
T [K]	20	10	5
q (H_2) $\left[\frac{\text{Torr}\cdot\text{l}}{\text{s}\cdot\text{cm}^2}\right]$	10^{-12}	10^{-13}	10^{-14}
Pressure Profile $P(x)$			
P_f [Torr]	2.1×10^{-12}	2.1×10^{-13}	2.1×10^{-14}
P_0 [Torr]	5.5×10^{-09}	5.5×10^{-10}	5.5×10^{-11}
ρ_{avg} $[H_2/\text{cm}^3]$	3.0×10^{7}	3.0×10^{6}	3.0×10^{5}
Wave Propagation			
Case I			
Q_t [Torr-l]	2.69×10^{-4}	2.65×10^{-4}	2.61×10^{-4}
t [years]	0.004	0.13	1.60
Case II			
Q_t [Torr-l]	2.69×10^{-2}	2.65×10^{-2}	2.61×10^{-2}
t [years]	0.42	13.18	159.82
Case III			
Q_t [torr-l]	6.73×10^{-2}	6.63×10^{-2}	6.53×10^{-2}
t_f [years]	1.05	32.96	399.55

OVERVIEW

First evaluations of the vacuum level and stability for the cold sections of the EIC HSR beamlines show promising results. The studies are based on COLDEX data. Several tests are planned to quantify and validate critical vacuum properties of the EIC beam screen at room and cryogenic temperatures. Ambient vacuum properties can have implications for the pre-cooldown process adopted for EIC as well as the pumping system design. The cryogenic vacuum properties can have implications on the screen design, including cross section shape, required contact pressure and thermal conductance, perforations and additional installed cryosorber capacity. The conclusions here presented will be reviewed once data for the EIC beam screen is available.

ACKNOWLEDGEMENTS

The authors would like to thank Wolfram Fischer, Steve Peggs and Henry Lovelace III for useful discussions.

REFERENCES

[1] F. Willeke *et al.*, "Electron-Ion Collider Conceptual Design Report", Brookhaven National Laboratory, Upton, NY, USA, Rep. BNL-221006-2021-FORE, Jan. 2021.

ISBN: 978-3-95450-214-1 ISSN: 2673-5490 doi:10.18429/JACoW-IPAC2021-WEPAB189

[2] S. Verdú-Andrés *et al.*, "A Beam Screen to Prepare the RHIC Vacuum Chamber for EIC Hadron Beams: Requirements and Conceptual Design", presented at the 12th Int. Particle Accelerator Conf. (IPAC'21), Campinas, Brazil, May 2021, paper TUPAB260, this conference.

[3] M. J. Rhoades-Brown and M. Harrison, "Vacuum Requirements for RHIC", Brookhaven National Laboratory, Upton, NY, USA, Rep. AD-RHIC-1-142, Dec. 1991.

[4] K. Mernick, M. Blaskiewicz, and J. M. Brennan, "Full 3D Stochastic Cooling at RHIC", in *Proc. North American Particle Accelerator Conf. (NAPAC'13)*, Pasadena, CA, USA, Sep.-Oct. 2013, paper MOZAA2, pp. 41–45.

[5] W. Fischer *et al.*, "Electron cloud observations and cures in RHIC", in *Proc. 22nd Particle Accelerator Conf. (PAC'07)*, Albuquerque, NM, USA, Jun. 2007, paper TUXAB02, pp. 759–763.

[6] R. Salemme, V. Baglin, G. Bregliozzi, and P. Chiggiato, "Vacuum Performance of Amorphous Carbon Coating at Cryogenic Temperature with Presence of Proton Beams", in *Proc. 7th Int. Particle Accelerator Conf. (IPAC'16)*, Busan, Korea, May 2016, paper THPMY007, pp. 3663–3666.

[7] J. P. Hobson and K. M. Welch, "Time-dependent helium and hydrogen pressure profiles in a long, cryogenically cooled tube, pumped at periodic intervals", *J. Vac. Sci. Technol. A*, vol. 11, pp. 1566–1574, 1993. doi:10.1116/1.578506